REPORT NO. NADC-87036-60

AD-A196 790

MICRODAMAGE IN SLIDING CONTACTS

DTIC
ELECTE
JUL 2 6 1988
S D
&D

Paul J. Kennedy
Air Vehicle and Crew Systems Technology Department
NAVAL AIR DEVELOPMENT CENTER
Warminster, Pennsylvania 18974

FEBRUARY 1987

FINAL REPORT
AIRTASK NO. A-320-320A/001-B/1F61-5442-000
WORK UNIT ZM510

Approved for Public Release; Distribution is Unlimited.

Prepared for
Naval Exploratory Development Program
Airborne Materials
NA2A
NAVAL AIR DEVELOPMENT CENTER
Department of the Navy
Warminster, PA 18974

SECURITY CLASSIFICATION OF THIS PAGE

REPORT DOCUMENTATION PAGE

1a REPORT SECURITY CLASSIFICATION Unclassified	1b RESTRICTIVE MARKINGS
2a. SECURITY CLASSIFICATION AUTHORITY	3 DISTRIBUTION / AVAILABILITY OF REPORT Approved for public release; Distribution is Unlimited.
2b DECLASSIFICATION / DOWNGRADING SCHEDULE	
4. PERFORMING ORGANIZATION REPORT NUMBER(S) NADC-87036-60	5 MONITORING ORGANIZATION REPORT NUMBER(S) N/A
6a NAME OF PERFORMING ORGANIZATION Naval Air Development Center 6b OFFICE SYMBOL (If applicable) 6061	7a NAME OF MONITORING ORGANIZATION N/A
6c. ADDRESS (City, State, and ZIP Code) Warminster, PA 18974	7b. ADDRESS (City, State, and ZIP Code) N/A
8a. NAME OF FUNDING / SPONSORING ORGANIZATION Naval Air Development Center 8b OFFICE SYMBOL (If applicable) 6062	9 PROCUREMENT INSTRUMENT IDENTIFICATION NUMBER
8c. ADDRESS (City, State, and ZIP Code) Warminster, PA 18974	10 SOURCE OF FUNDING NUMBERS PROGRAM ELEMENT NO: 62234N PROJECT NO: RS34A52 TASK NO: A-320-320A/001-B/1F61-542-000 WORK UNIT ACCESSION NO: ZM510

11 TITLE (Include Security Classification)

(U). Microdamage in Sliding Contacts

12 PERSONAL AUTHOR(S) Paul Kennedy

13a TYPE OF REPORT	13b TIME COVERED	14 DATE OF REPORT (Year, Month, Day)	15 PAGE COUNT
Final	FROM _____ TO _____	February 1987	20

16 SUPPLEMENTARY NOTATION

17 COSATI CODES		
FIELD	GROUP	SUB-GROUP
11	08	

18 SUBJECT TERMS (Continue on reverse if necessary and identify by block number)

Fretting, Tests, Metal, Microslip, Wear, Friction, Carbon Steel

19 ABSTRACT (Continue on reverse if necessary and identify by block number)

Studies based on subjecting a ball-on-flat test specimen configuration to small amounts of slip (0 to 5 μm) suggest a possible mechanism for the initiation of surface damage and wear. This study, which was limited to SAE 52100 steel, indicated that a significant number of transitions occurred in the initiation of the fretting process. These transitions, in order of severity, included initially mild oxidation, minimal surface damage, and a mild to severe wear process characterized by a pitted wear surface, tensile stress cracking and microcrack formation. An SEM analysis of the Hertzian contact region under load indicated a significant surface roughening was found to correspond approximately to the size of carbide particles. This suggests that carbides, due to their higher modulus, might protrude out of the surface under load and thus alter surface morphology in the ball/flat contact region. This change in surface morphology in the contact area could explain all of the various types of surface damage observed in this study. Data suggests that accelerated wear could be explained on the assumption that carbide particles could work free of the surface under high surface stress conditions and that these freed particles could then accelerate wear by acting as an abrasive in the contact zone.

20 DISTRIBUTION / AVAILABILITY OF ABSTRACT	21 ABSTRACT SECURITY CLASSIFICATION
☐ UNCLASSIFIED/UNLIMITED ☐ SAME AS RPT ☐ DTIC USERS	Unclassified
22a NAME OF RESPONSIBLE INDIVIDUAL Paul Kennedy	22b TELEPHONE (Include Area Code) (215) 441-1567 22c OFFICE SYMBOL 6062

DD FORM 1473, 84 MAR 83 APR edition may be used until exhausted
All other editions are obsolete

SECURITY CLASSIFICATION OF THIS PAGE

U.S. Government Printing Office: 1985—607-047

TABLE OF CONTENTS

Accesion For
NTIS CRA&I
DTIC TAB
Unannounced
Justification
By
Distribution/
Availability Codes
Dist
A-1

LIST OF ILLUSTRATIONS

INTRODUCTION

Sliding surface damage can occur under extremely small amplitude slip conditions. The primary difference in damage resulting from small amplitude fretting type motions, as compared to gross sliding, is in the degree or severity of surface damage. Fretting wear is usually mild and produces a fine oxidized form of wear debris. Wear coefficients reflect this and are usually small and of the order of 10 exp −7 to 10 exp −9. Gross sliding, on the other hand, is commonly associated with much larger wear particles and wear coefficients that are several orders of magnitude greater than those observed in low amplitude fretting. In a previous study of extremely small amplitude slip (0 to 5 μm) on the fretting of SAE 51200 steel(1), surface damage in the wear scar region, although partially hidden by debris, was minimal. This general absence of surface damage allowed the observation of several interesting transitions in the fretting wear process that included initially mild oxidation or staining, followed by a mild polishing type of wear process. At higher amplitude slip, wear was more abrsasive and characterixed by microcrack formation in the wear region. In addition to these reported changes in surface morphology as a function of slip amplitude, an elastic analysis of the wear scars indicated that the coefficient of friction for SAE 52100 steel would need to be approximately 1.5 in order to elastically account for observed change in wear scar dimensions as a function of applied slip amplitude.

The primary objective in this study was to determine what factors were responsible for the development of the unusual wear scar patterns that were observed in the previous study(1). The approach consisted of conducting experiments that would elucidate surface damage mechanisms operating at small amplitude slip and would also clarify what factors were responsible for the predicted high coefficient of friction. This coefficient of friction was based on an elastic analysis developed by Deresiewicz(2) for two elastic spheres subjected to an oscillating torsional couple. A possible reason that might account for the predicted high coefficient of friction would be the inability of this model to account for the effect of wear debris in the contact zone.

In the previous studies(1,3) a profuse amount of dark red wear debris was observed in the wear area even though extremely small slip amplitudes were used in testing. The minimal surface damage that would be expected with low amplitude slip was offset in the previous experiments(1,3) since the duration of test was relatively long. Testing exceeded over 2.3 million stress cycles. In the case of a ball on flat configuration, this wear debris, in addition to hiding scar characteristics, would be expected to alter the normal stress distribution across the ball/flat contact area and this factor could then change the wear scar dimensions. These dimensions in turn, formed the basis of the elastic analysis. An alternate hypothesis that could account for a very high coefficient of friction would require the assumption that the surface morphology in the contact zone changes under load. Under sufficiently high pressures, carbides particles might protrude from the surface and alter the lubricating characteristics of the oxide film. The intent of this study was to test these hypotheses and to determine factors responsible for the transitions observed in the fretting process at low amplitude slip.

BACKGROUND

The objective of the previous investigation(1) was to determine the minimum slip amplitude associated with surface damage so that this could be incorporated in future aircraft design work. The intent of this investigation was to study the mechanism responsible for the fretting of SAE 52100 steel by correlating applied slip amplitude with type of surface damage. Relatively little work has been done on the effect of extremely small slip amplitudes (i.e., 0 to 10 μm) on fretting. Most of the undertakings in this region were concerned with evaluating the elastic and plastic behavior of materials. Some of the work in this region and other work at higher amplitude slip were related to the determination of the extent of fretting damage as a function of slip amplitude. For example, the upper limit of motion was estimated by Halliday(4) and Ohmae and Tsukizoe(5) as being approximately 250-300 μm. Beyond this length, the fretting wear process would change to wear more typical of unidirectional sliding. The lower limit or the minimum amount of slip necessary to produce fretting is more difficult to define. In the case of two contacting bodies, a certain amount of the applied motion would be taken up elastically and the remainder of the applied motion would be taken up as slip. This relative or elastic microdisplacement would be greater than zero and would have a maximum value equal to that produced by a tangential force just less than that of limiting friction(6). Thus, fretting would require microdisplacements in excess of this minimum value. Johnson(6) in very accurate work, measured elastic microdisplacement values of 1 to 3 μm preceding large scale slip for steel on steel. Courtney-Pratt and Eisner(7) reported similar data and also showed that the displacement necessary to produce slip was decreased in the presence of lubricant. The exact value for the amount of elastic deformation that preceeds slip would, of course, be dependent upon experimental conditions. In the previous study(1) we reported a value of 0.06 μm for the minimum slip amplitude associated with oxidative damage. Surface staining was observed at this applied slip amplitude. This value of 0.06 μm was measured at the low pressure edge of the wear scar where elastic deformation would be minimal and would thus indicate the actual amount of slip necessary to produce the first evidence of fretting. This value is significantly greater than the value of 0.002 μm as reported by Tomlinson(8). Sato et. al.,(9) using a steel ball and glass flat configuration reported visual evidence of surface damage at a slip amplitude of 4 μm. The minimum slip amplitude associated with surface damage was not evaluated in the above study.

EXPERIMENTAL

APPARATUS AND PROCEDURES

The test specimen configuration used in this study is shown in Fig. 1. The ball specimens were standard grade 25 E.P. 12.7-mm SAE 52100 steel balls. The flats were machined from SAE 52100 steel and were heat treated to a final hardness of Rc 64. Flat specimens were then hand polished using 0.3 and 0.05-um alumina. Both the ball and flat specimens were washed in boiling stoddard solvent and rinsed in petroleum ether prior to testing. The test specimens were then inserted into a fretting test rig under 9 kg load. This test rig was previously described(1). Most conventional wear test devices using a ball on flat type of specimen arrangement would normally generate fretting wear by imparting a linear oscillatory motion to one of two contacting specimens under load conditions. The length of this back-and-forth displacement would be defined as the slip amplitude. Alternately, a similar type of fretting motion can be produced by using an angular displacement rather than a linear displacement. Loading of a ball against a flat, as shown in Fig. 1, produces a circular Hertzian contact region which defines the actual damage or wear area. Under normal test conditions, the contact area would have a radius of approximately 0.15 mm. During testing, the ball specimen is held stationary and an oscillatory twisting type of motion through an angle, theta, is imparted to the flat specimen. This motion was about the Z-axis which is normal to and through the center of the ball/flat contact region. The slip amplitude at the edge of the ball/flat contact area can be easily calculated knowing the magnitude of the angle of twist and the radius of the contact area. The primary experimental variables were the angle of twist or slip amplitude, the normal load and the duration of test. Duration of test was one of the primary experimental variables analyzed in this study. In previous testing, fretting specimens were analyzed after 2.3 million fretting cycles. In this study, the majority of test specimens were analyzed after 12,600 fretting cycles.

WEAR SCAR ANALYSIS

A typical wear scar, resulting from the oscillatory torsional motion of a ball against a flat, is illustrated in Fig. 2. The outer diameter of the wear scar can be calculated using the Hertz equations. The inner diameter would be dependent on normal and shear stresses. This can be seen by considering a ball resting on a flat plate under elastically loaded conditions. This will produce a normal stress distribution over the ball/flat contact area. This stress would be zero at the edge of the contact and a maximum in the center. Application of a shearing or twisting force to the flat produces a shear stress distribution that would have a maximum near the edge of the contact area and a minimum in the center. Estimates of the shapes of these distributions are shown in Fig. 2. The action of these two opposing forces can produce relative motion or sliding in the Hertzian contact region.

Relative motion or sliding requires that the applied shearing force must exceed the product of the static coefficient of friction and the normal load. The inner dash lines in Fig. 2 represent a radius which can be defined as the locus of those points at which the ratio of the shear to normal stress is exactly equal to the static coefficient of friction. Thus, relative motion or sliding can only occur at radii greater than the inner radius shown in Fig. 2 or outside of the inner dash line region. This region is called the slipped region. Inside of the dash line region in Fig. 2 or in the central region of the contact area, the converse will hold true and the shearing force will always be less than the product of the normal stress and coefficient of friction and thus, all motion will be taken up elastically. This is normally referred to as the locked region.

Slip can not be directly calculated along the radius of the wear scar using the applied angle of twist. At the edge of the locked region, no motion can occur since all applied motion will result in elastic deformation. Elastic deformation effects must also be taken into consideration at all other points in the wear scar region except at the edge of the slipped region. At this point the normal stress is equal to zero and no elastic deformation can occur. In this paper, slip was calculated at the edge of the Hertzian contact region.

RESULTS AND DISCUSSION

Wear scars, similar to those predicted on the basis of the elastic analysis in Fig. 2 are shown in Fig. 3. Both the locked or inner circular region and the slipped or the outer ring region can be seen in each of these photos. The absence of surface damage in the locked region can be seen in photomicrograph (a) since small surface scratches in the locked region were not obliterated during testing. These wear scars were formed by loading a 12.7 mm diameter SAE 52100 steel ball against a SAE 52100 flat under 9 kg load and subjecting the ball/flat combination to an oscillatory twisting type of motion equivalent to the amount of slip indicated under each photo in Fig. 3. Similar wear scars were formed on the SAE 52100 ball specimens. The outer diameter of these scars are approximately 0.3 mm and correspond to that which would be predicted on the basis of the Hertz equation. The slip amplitudes indicated under each of the photomicrographs in Fig. 3 were calculated at the Hertz radius from the angle of twist. These wear scars, although they were part of a previous study (1), clearly illustrate some of the changes in wear scar characteristics that are slip amplitude dependent. Photo (a) shows that surface straining or very mild oxidation can occur at a slip of 0.1 um. Based on this measurement and wear tests at lower amplitudes, the minimum amount of microslip capable of producing surface oxidation or straining was estimated at approximately 0.06 μm. Surface profile measurements indicated that the amount of surface damage was minimal in photos (a) and (b) but significant in photo (c). This later photo also shows a ring of wear debris around the wear scar. This data indicates that considerable surface damage can occur at slip amplitudes as small as 2.5μm.

The results of a previous analysis of these wear scars using the elastic model developed by Deresiewics(2) indicated that the observed decrease in the radius of the locked region with increased applied shear stress or slip would require a static coefficient of friction of 1.5. A value of 0.4 to 0.8 would seem more reasonable for steel on steel, but it was also pointed out that this value represents a static coefficient of friction occurring under high pressure conditions on a surface where relative slip had not previously taken place(1). Another difficult to explain phenomena was the occurrence of a thin polished band at higher amplitude slip. This phenomenon can be seen in photo (d) of Fig. 3. This photo is characterized by four distinct wear regions consisting of (1) a locked region, (2) a roughened inner ring region characterized by what appears to be a roughened surfaced, (3) a thin polished band and (4) a very dark outer ring consisting of wear debris. Photo (d) also illustrates a clearly defined transition from an initial wear process responsible for the development of a roughened inner ring to a second wear process responsible for the development of a polished band. Theory would indicate that all wear processes would be limited to that area defined by the slipped region (i.e., that area in which the shear force exceeds the product of the coefficient of friction times the normal force) and would not suggest any reasons to account for any abrupt wear transitions in this region. A third finding, which was not completely explained, was the development of fine microcracks in the slipped region. These cracks or grooves can be seen in Fig. 4. They are oriented perpendicular to the direction of slip which suggested the onset of fatigue(10).

The lack of good explanations for these findings prompted further study of the effect of low amplitude slip on the fretting process. The primary emphasis in our more recent work was to determine if the presence of wear debris in the inner ring region might influence the normal stress distribution in the ball/flat contact region. For example, wear debris that collects near the edge of the wear scar could result in a pressure spike in the normal stress distribution and this could possibly result in the formation of an additional locked area. With this in mind, a series of fretting experiments were conducted at very short durations with the intent of eliminating or greatly reducing the effect of wear debris. Photomicrographs from this study are shown in Fig. 5. These wear specimens were limited to 12,600 fretting cycles to reduce wear particle build-up. The general absence of wear debris in these photomicrographs also has the advantage of clearly showing topographical features that were not evident in the previous study. Photo (a) shows a typical wear scar formed under low amplitude slip for a short test duration. This wear scar consists of an oxide ring corresponding to the outer diameter of the Hertzian contact region. Surface profile measurements did not indicate any measurable surface damage. The wear scar in photo (b) was produced at a higher slip amplitude and shows evidence of surface roughening not seen in the photo (a). This surface roughening consists of small depressions and raised areas. Photo (c) at still higher amplitude slip shows evidence of the development of a thin polished band between the roughened inner ring and an outer ring consisting of extruded wear debris.

Amplitudes larger than those shown in Fig. 5 were found to produce wear scars that showed unusual and difficult to explain surface characteristics. These scars show the same undamaged region and three distinct wear regions that were previously noted in Fig. 3 but with much better resolution. These regions are numerically labeled in photo (a) of Fig. 6. Region 1 is the locked region that would be expected on the basis of elastic theory. Surface texture in this region is identical to the undamaged surface of the flat outside of the contact zone. Regions 2 and 3 combined form the slipped region. Region 2 can be seen as distinct from region 3. It forms a relatively wide, rough region that has the appearance of an inner ring. Region 3 which is actually a very thin polished band, is clearly visible at 500X magnification in photo (a). Region 4 defines the outer edge of the wear scar. In this region, photo (a) shows that the wear debris is in the form of a very thin extruded sheet of material. This wear debris partially hides a groove that forms a ring around the wear region. This last region can be called a ring groove region.

The inner ring or region 2 can be seen more clearly in Fig. 6, photo (b) using different illumination. Close examination of photo (b) suggests the presence of numerous elongated holes. These holes also appear to be in an axial direction or elongated in the direction of slip. This was not observed in the previous study(1) since the larger part of that work involved testing in excess of 2 million fretting cycles. Only 12,600 cycles were used in this study. Long testing would be expected to result in the obliteration of this pitted appearance. Region 3 is not highly visible in photo (b). The remaining two photomicrographs in Fig. 6 focus on the morphological features of region 2 and 3. Photo (c) is the same wear scar taken at an oblique angle. This photo shows the morphology of the wear scar and indicates the general area shown in photo (d). This last photo shows a close-up of the polished region taken at an oblique angle. This thin polished band, shown in the middle region of photo (d), can be seen as a region in which the metal surface has been flattened or polished smooth. This suggests that considerable slip had occurred in this third region. This division of the slipped region into two distinct wear regions may be related to normal and sheer stress distributions in that region 2 is a low slip, high stress while region 3 is a high slip, low stress area.

Ring groove formation (region 4) is more clearly seen in Fig. 7. The photomicrographs are wear scars generated at 4.3 μm. Photos (a), (b) and (c) are of wear scars formed after 126,000 fretting cycles; photo (d) represents 378,000 cycles. Photo (a) shows extrude wear debris over the groove. Higher magnification photos in (b) and (c) shows the contour of the groove. The inner side of the ring groove in photo (c) can be seen to be fairly steep. This ring groove represents an interesting phenomenon and can be probably attributed to the interaction of a torsional force with the tensile stresses (0.13 maximum pressure) existing outside of the Hertzian contact region. This ring groove is amplitude dependent. This dependency was quantified by nital etching of test specimens. Examination of test specimens generated at different slip amplitudes after nital etching indicated that the ring groove first developed at a slip amplitude of approximately 1.9 μm under a 9 kg load. Studies of the effect of time on ring groove development suggest that the outer diameter of the groove increases with time. The groove, in turn, tends to collect the wear debris extruded out of the contact region. This debris can be seen at the bottom of the ring groove in photo (d). Examination of wear scars formed after 2,000,000 or more fretting cycles indicates that the ring groove will eventually become completely filled with extruded wear debris.

The general contour of the damaged region can be seen in Fig. 8. Some of these characteristics are slip amplitude dependent while others are time dependent. At slip amplitudes less than 0.06 μm, no damage occurs. For slip amplitudes up to 1.4 μm, surface staining occurs in the slipped region. The fourth region, the ring groove region, appears at 1.9 μm. The slipped region divides into regions 2 and 3 at a slip amplitude of about 2.8 μm. In addition to slip amplitude dependent characteristics, two time dependent parameters were also observed. These time dependent characteristics were observed by conducting fretting cycles. The first time related characteristic, the widening of the ring groove with time, was previously mentioned. The other characteristic, which was previously interpreted as microcracks or fatigue formation, can be seen in Fig. 4. In this figure, region 3 or the thin polished band region is no longer polished but exhibits a washboard type of surface. This effect was not observed until after 390,000 fretting cycles. Although these microcracks have the correct orientation for fatigue crack formation, closer observation indicates that the cracks are shallow and their occurrence in the polished region suggests that the cracks may have been gorged out by hard particles extruded out from the inner ring region under the influence of the pressure gradient.

One common explanation that would explain (1) a high theoretical value for the static coefficient of friction, (2) two different wear processes occurring in the slipped region, (3) the development of elongated holes in the inner ring or region 2 and finally (4) the washboard effect found in the thin polished band of the slipped region should provide a clue to the mechanism responsible for low amplitude fretting damage. Since SAE 52100 steel is a physical mixture of hard carbide particles embedded in a softer iron matrix, then the application of high pressures could cause protrusion of carbides from the surface. This effect was investigated by loading a ball against a flat using a simple loading device consisting of an upper plate machined to hold the ball specimen and a lower plate machined to hold the flat specimen. Load was applied by tightening the bolts used in joining the two plates. This device and test specimens, at 2X magnification, are shown in Fig. 9.

This photo was taken after the device and test specimens were metallurgically mounted, sectioned transversely and polished down to exposed the Hertzian contact region. Photomicrographs of the cross-sectioned ball on flat under actual load conditions are shown in Fig. 10. These photos at 14X and 140X indicated a significant surface roughening effect. Photographs, not shown in this report but at much higher magnification, indicated that this roughening corresponded to particles about 1.3 μm in size which would correspond to the 1.0 μm particle size expected for carbides in SAE 52100. Higher magnification studies of this region also showed two cracks, which may be responsible for the initiation of ring groove formation, oriented perpendicular to the surface and most probably located at the edge of the Hertzian contact region. These tensile cracks are shown in photos (a) and (b) of Fig. 11.

Fig. 12 is a composite plot of the pressure distribution and estimates of the amounts of slip occurring in the ball/flat contact area for applied slip amplitude of 1.9 and 3.8 μm (i.e., applied at the Hertz radius). Both pressure and slip are plotted as a function of (a), the contact radius. Region I is the locked region, observed in actual wear scars, which would be characterized by extremely high pressures and little if any slip. Regions II and III would encompass the observed wear region. Region II is a high pressure region. In this region, pressures would be sufficient to cause the carbides to protrude from the mating surfaces and cause an interlocking of the ball with the flat. This would negate the effect of the oxide film and account for the high static coefficient of friction. If a small fraction of the carbide particles on the surface of the flat are envisioned as penetrating the softer steel matrix of the ball, then an oscillating torsional type of motion might result in dislodging the particles from the surface. This would require a certain slip threshold at least a few lengths greater than the diameter of the particle, itself. For example, in the case of experiments run at 1.9 μm, slip in region II might be expected to elastically deform the matrix around the carbide but would probably not be sufficient to result in freeing of the carbide. At 3.8 μm, sufficient plastic deformation of the steel matrix might occur so as to allow the particles to work free of the surface. This would account for the observed elongated holes. The particles would then act as an abrasive causing considerable surface damage. This damage would be limited by the pressure gradient over the contact area which would tend to force the migration of carbide grains out of region II.

In region III, pressures are not sufficient to cause matrix deformation and thus the abrasive wear, characteristic of region II can not occur. The large amplitude slip in this region accounts for the observed polishing action. With time the carbide particles would be extruded through this region and possibly cause the observed washboard effect. Region IV, which actually lies outside of the contact region, is a region characterized by moderately high tensile stress. For 9 kg load, this corresponds to 40,000 psi. This stress would account for the tensile cracks observed in the photomicrographs of Fig. 11. The combination of this stress with the torsional stress could account for ring groove formation.

For the most part, these observations were based on fretting tests that were designed to minimize the influence of wear debris on wear scar characteristics. The primary findings were based on the observation of morphological changes that were previous hidden by damage or accumulated wear debris. An original intent of this investigation was to determine the effect of wear debris on the pressure distribution. This effect was not as critical as previously believed. Data suggests that the radius of the locked region does decrease slightly with time, but that the radius will reach a constant value after approximately 750,000 fretting cycles. For example, visual inspection of a wear scar at 2 million cycles was found to be essentially identical to a wear scar formed after 4 million cycles. These and similar observations suggest that the wear scar does change slightly as a result of wear. The normal stress distribution appears to change in such a way that the maximum stresses are confined to the locked region. Once this occurs, the damage pattern will remain essentially constant.

CONCLUSIONS

An investigation into factors that might contribute to unusual wear scar characteristics and possibly contribute to a high value for the static coefficient of friction for SAE 52100 steel on itself suggests an unusual mechanism for fretting damage under low amplitude slip conditions. From the results of our experiments, the following conclusions can be made:

1. The surface oxidation observed at very low amplitude slip is the result of the polishing action of the rubbing surfaces. This can occur at slip amplitudes as small as 0.06 um.

2. Under high pressure conditions. The high modulus of carbide particles relative to the iron matrix results in the partial protrusion of carbides out of the surface.

3. Under the combination of high pressure and slightly higher amplitude slip conditions, carbide particles appear to work free of the surface as a result of high surface stresses. The freed carbides can then act as an abrasive and greatly accelerate the wear process. This accelerated wear can occur at slip amplitudes as low as 2.8 μm.

4. This same combination of conditions can lead to a tensile cracking failure that encircles the ball/flat contact area. This could lead to fretting fracture.

In summary, the three regions of damage which include (1) the inner ring region, (2) the polished ring region and (3) the ring groove region can be defined in terms of the relationships of normal stress to slip. This analysis was developed from the study of a ball on flat type configuration subjected to an oscillating torsional motion.

Similar results might be expected for extremely small slip amplitudes produced by a linear oscillatory type motion. In either event, high amplitude slip would negate the effect of carbide protrusion since surfaces would rapidly become worn and wear debris between the surface would retard this effect. This effect, however, might be of importance in rolling contact bearings.

REFERENCES

(1) Kennedy, P. J., Peterson, M. B. and Stallings, L., "A study of surface damage at low amplitude slip," ASLE Trans., 27, 4, pp 305-312 (1984).

(2) Deresiewicz, H., "Contact of Elastic Spheres under an Oscillating Torsional Couple," J./ Applied Mech., Trans. ASME, 76, pp 52-56 (1954).

(3) Kennedy, P. J., Peterson, M. B. and Stallings, L., "An Evaluation of Fretting at Small Slip Amplitudes," Materials Evaluation under Fretting Conditions, ASTM STP 780, American Society for Testing and Materials, pp 30-48 (1982).

(4) Halliday, J.S. and Hirst, W., "The Fretting Corrosion of Mild Steel," Proc. Royal Society (London), 236A, pp 411-425 (1956).

(5) Ohmae, N. and Tsukizoe, T., "The Effect of Slip Amplitude on Fretting," Wear, 27, pp 281-294 (1974).

(6) Johnson, K. L., "Surface Interaction between Elastically Loaded Bodies under Tangential Forces," Proc. Roy. Soc., A, 230, pp 531-548 (1955).

(7) Courtney-Pratt, J. S. and Eisner, E., "The Effect of Tangential Force on the Contact of Metallic Bodies," Proc. Roy. Soc., A, 238, pp 529-550 (1957).

(8) Tomlinson, G. A., "The Rusting of Steel Surfaces in Contact," Proc. Royal Society (London), 115A, pp 472-483 (1927).

(9) Sato, J., Shima, M., Igarashi, J., Tanaka, M. and Waterhouse, R. B., "Studies of Fretting (part 1)," Journal of JSLE International Edition, 3, pp 15-19 (1982).

(10) Collins, J. A., "Failure of Materials in Mechanical Design," John Wiley and Sons, New York, p 481 (1981).

(11) Waterhouse, R. B., "Fretting Wear," Proc. 1981 Intl. Conf., San Francisco, California, American Society of Mechanical Engineers, pp 17-22 (1981).

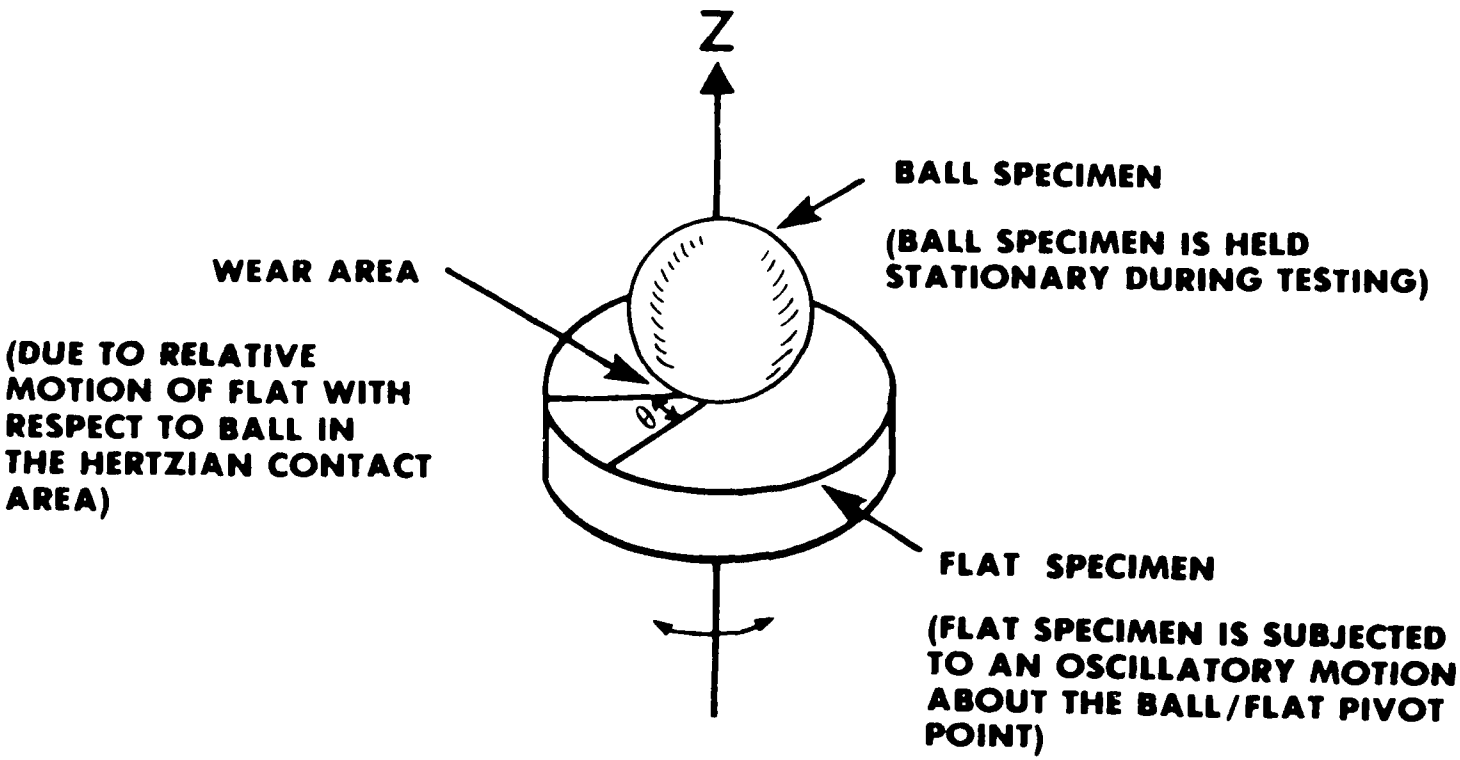

Figure 1 - Specimen configuration and relative motion of the ball against the flat.

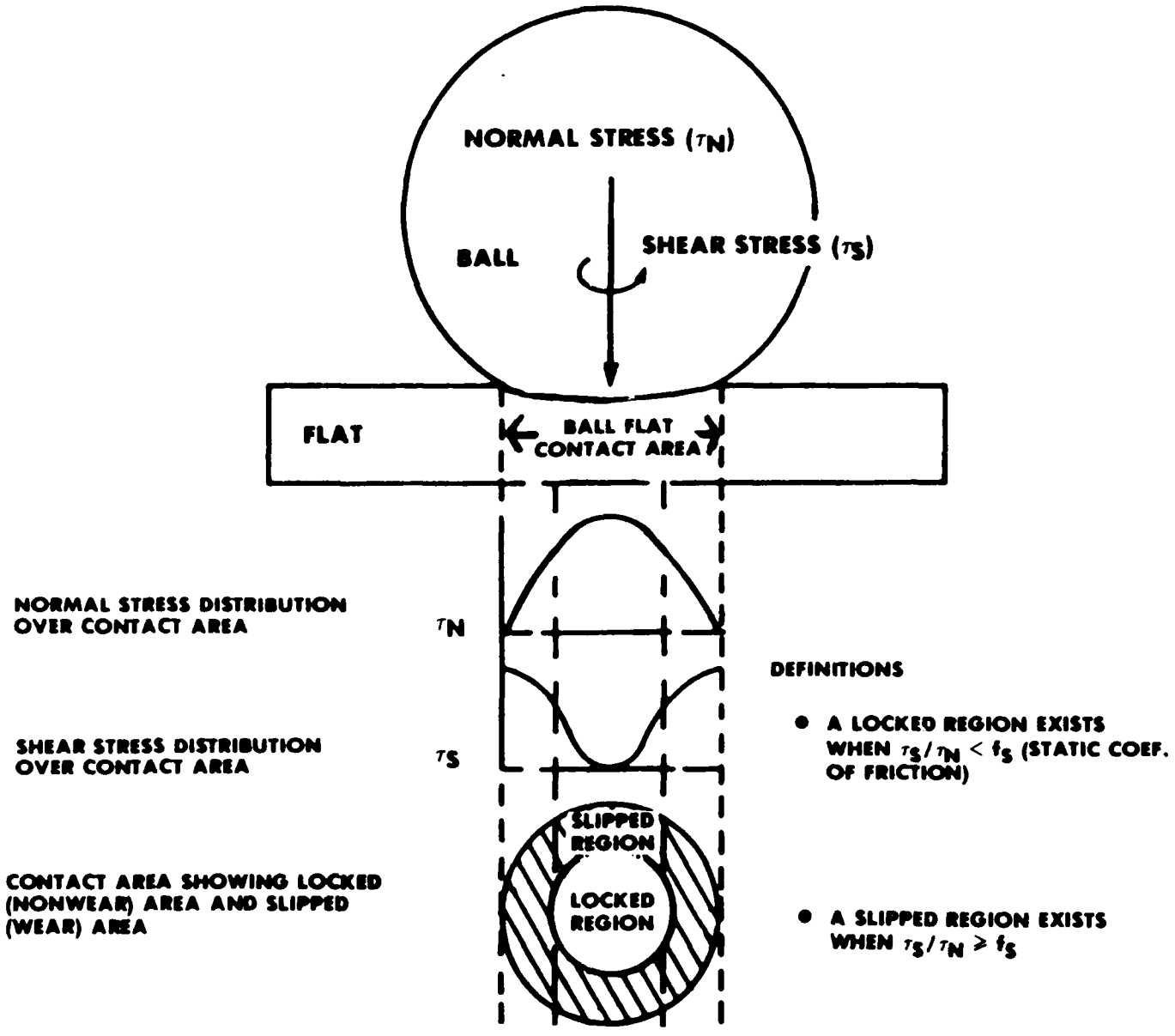

Figure 2 - Ball-on-flat configuration showing the relationship of shear stress, normal stress and coefficient of friction in determining wear scar dimensions.

(a) 0.1 μm SLIP (3 HOURS)

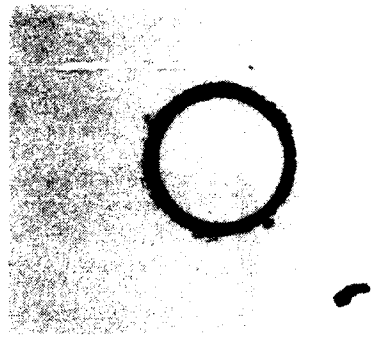

(b) 1.0 μm SLIP (3 HOURS)

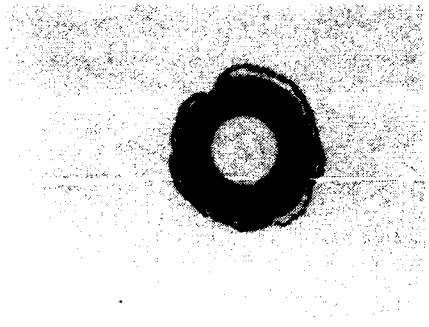

(c) 2.5 μm SLIP (3 HOURS)

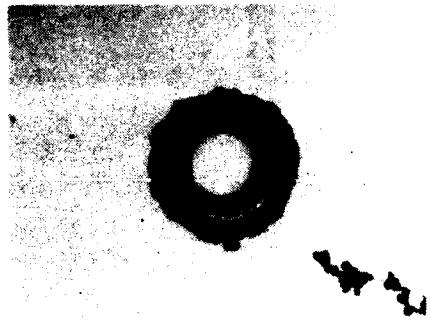

(d) 4.0 μm SLIP (1 MINUTE)

Figure 3 - Wear scars illustrating the effect of slip amplitude on scar dimensions and type of surface damage. Scars are on SAE 52100 steel flats at X100 magnification.

Figure 4 - Photomicrograph showing a time dependent wear scar characteristic that resembles microcrack formation.

(a) DAMAGE AT 1.43 μm SLIP (1 MINUTE)

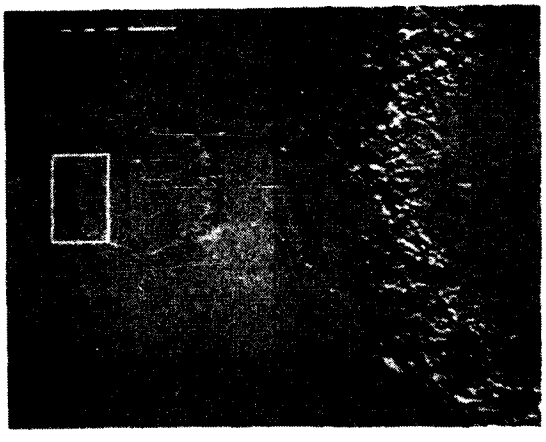

(b) DAMAGE AT 1.90 μm SLIP (1 MINUTE)

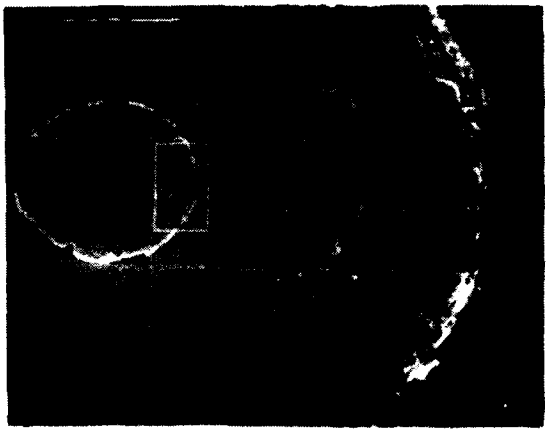

(c) DAMAGE AT 2.85 μm SLIP (1 MINUTE)

Figure 5 - Wear scars illustrating the development of surface damage under conditions of small amplitude slip.

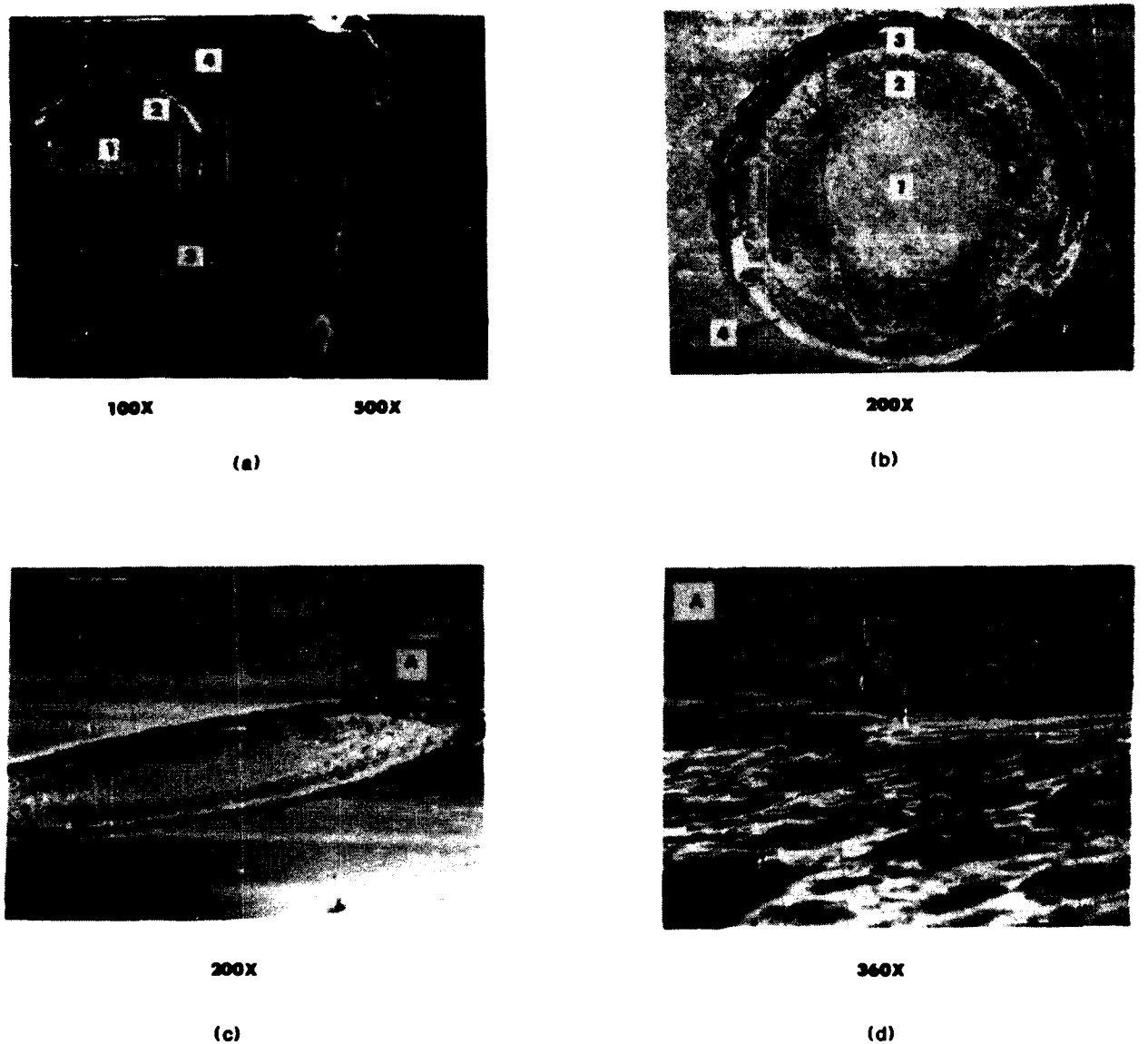

Figure 6 - Photomicrographs of wear scar formed at 3.8 μm slip which illustrate four numerically labeled wear scar regions that include (1)a locked region,(2) an inner ring, (3) a thin outer or polished ring and (4) a ring groove region.

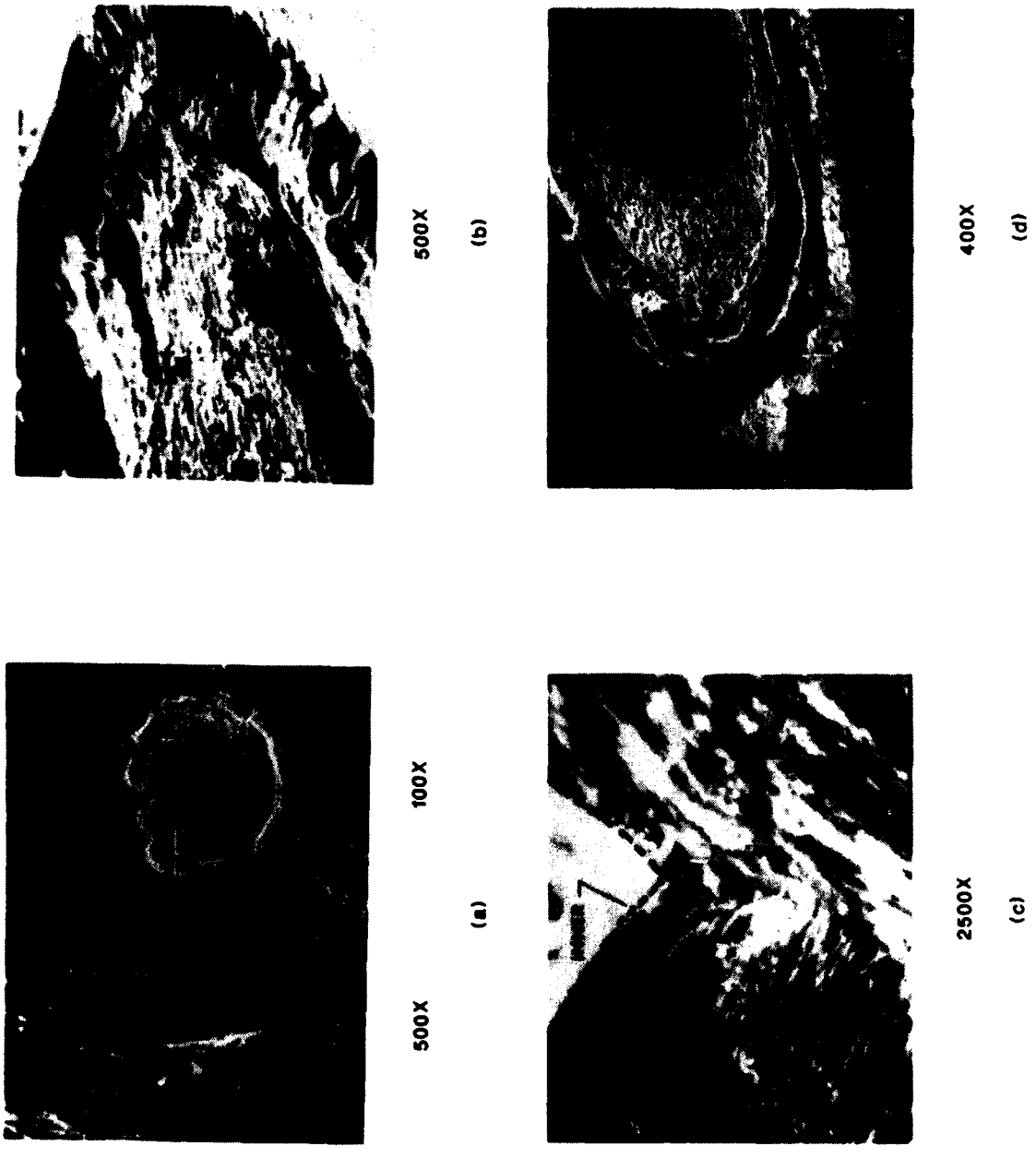

Figure 7 - Photomicrographs of wear scars formed at 4.3 μm slip showing region 4 or the ring groove region.

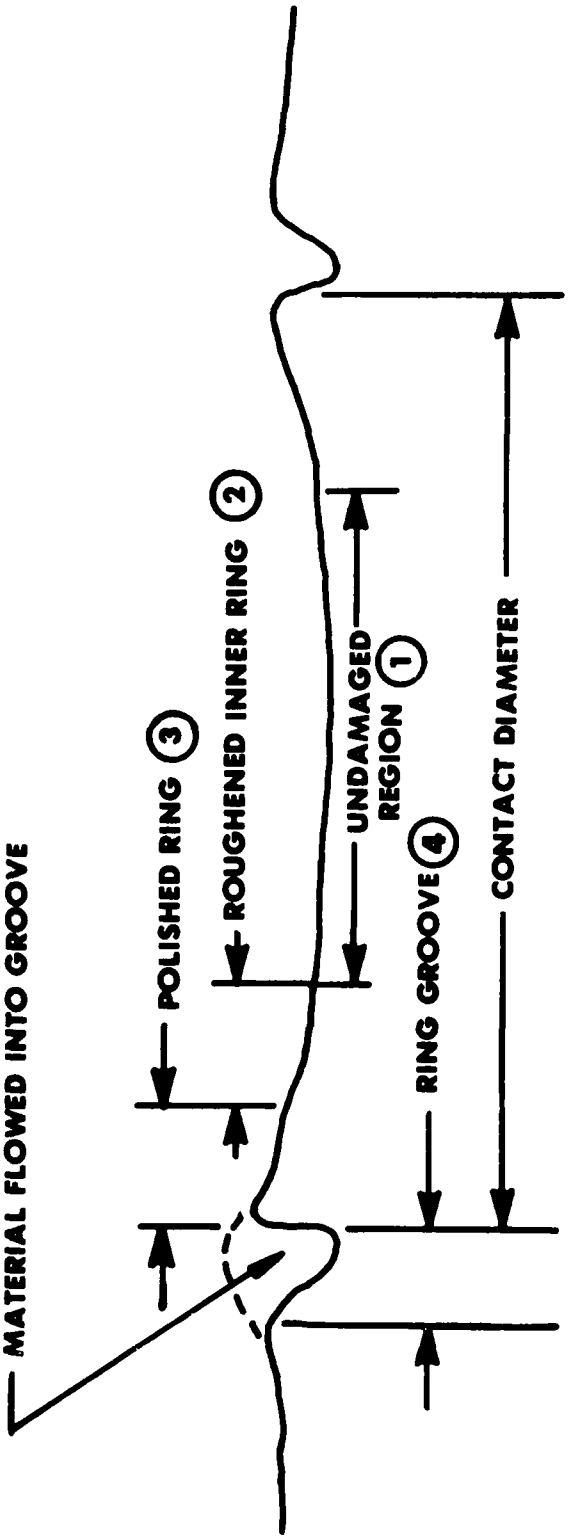

Figure 8 - A sketch of the general contour of the damaged region.

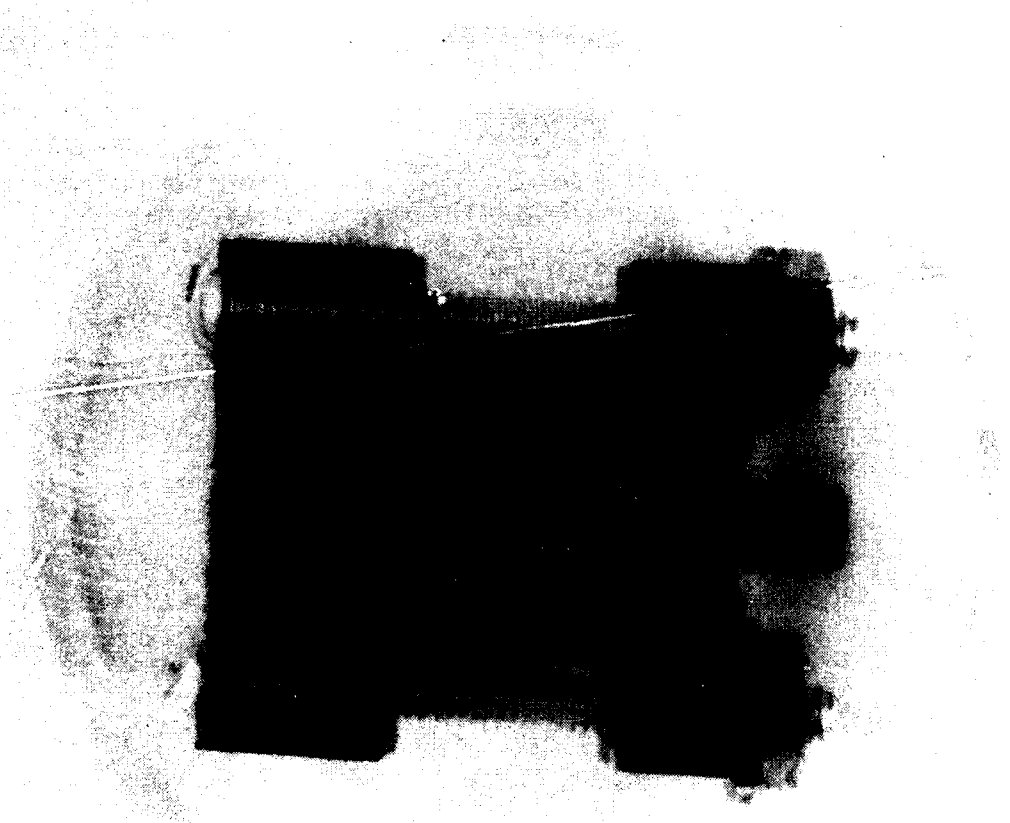

Figure 9 - Photograph of loading device and test specimens after metallurgically mounting and sectioning.

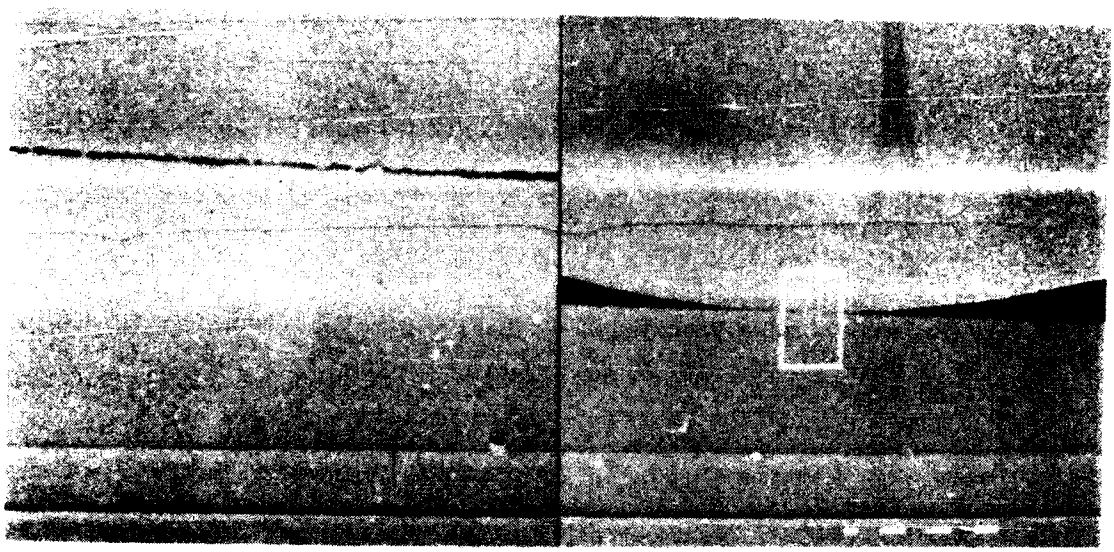

Figure 10 - Photomicrograph of cross-section ball-on-flat showing a surface roughening effect under an applied load.

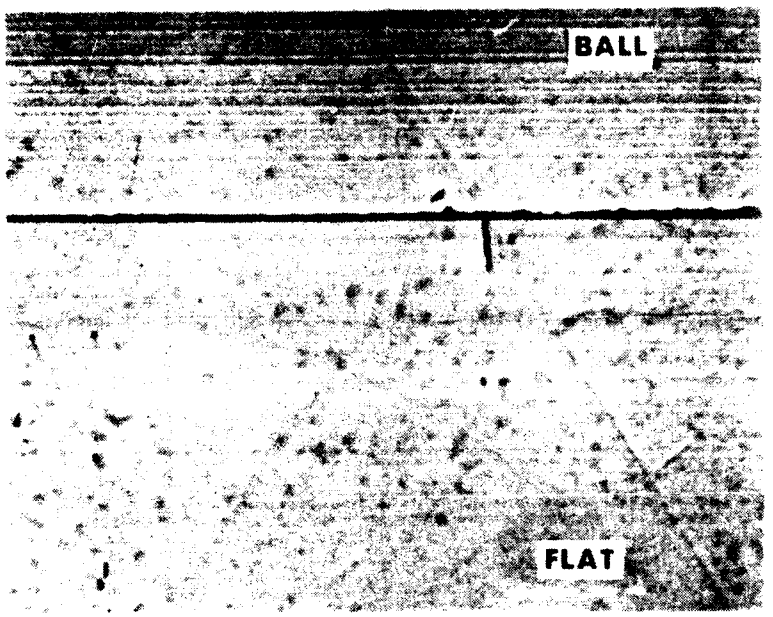

(a)

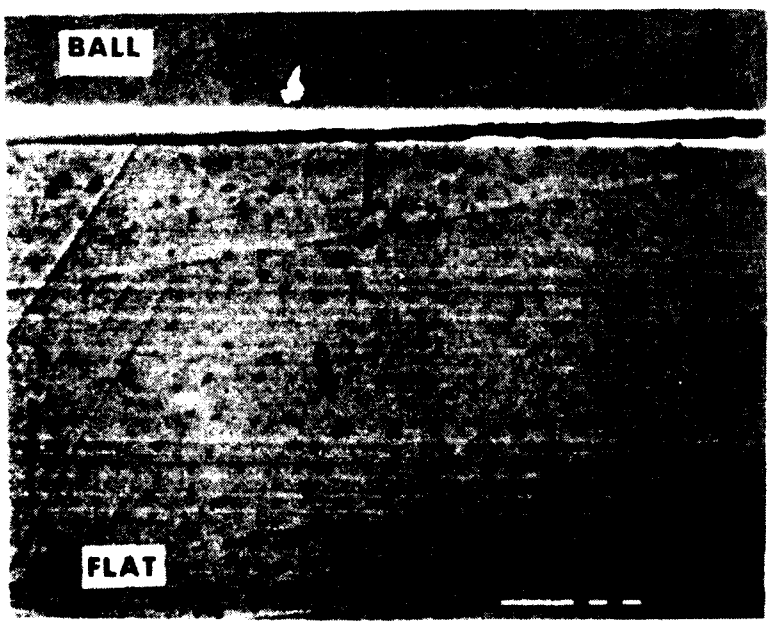

(b)

Figure 11 - Tensile stress cracks at the edge of the ball/flat contact area.

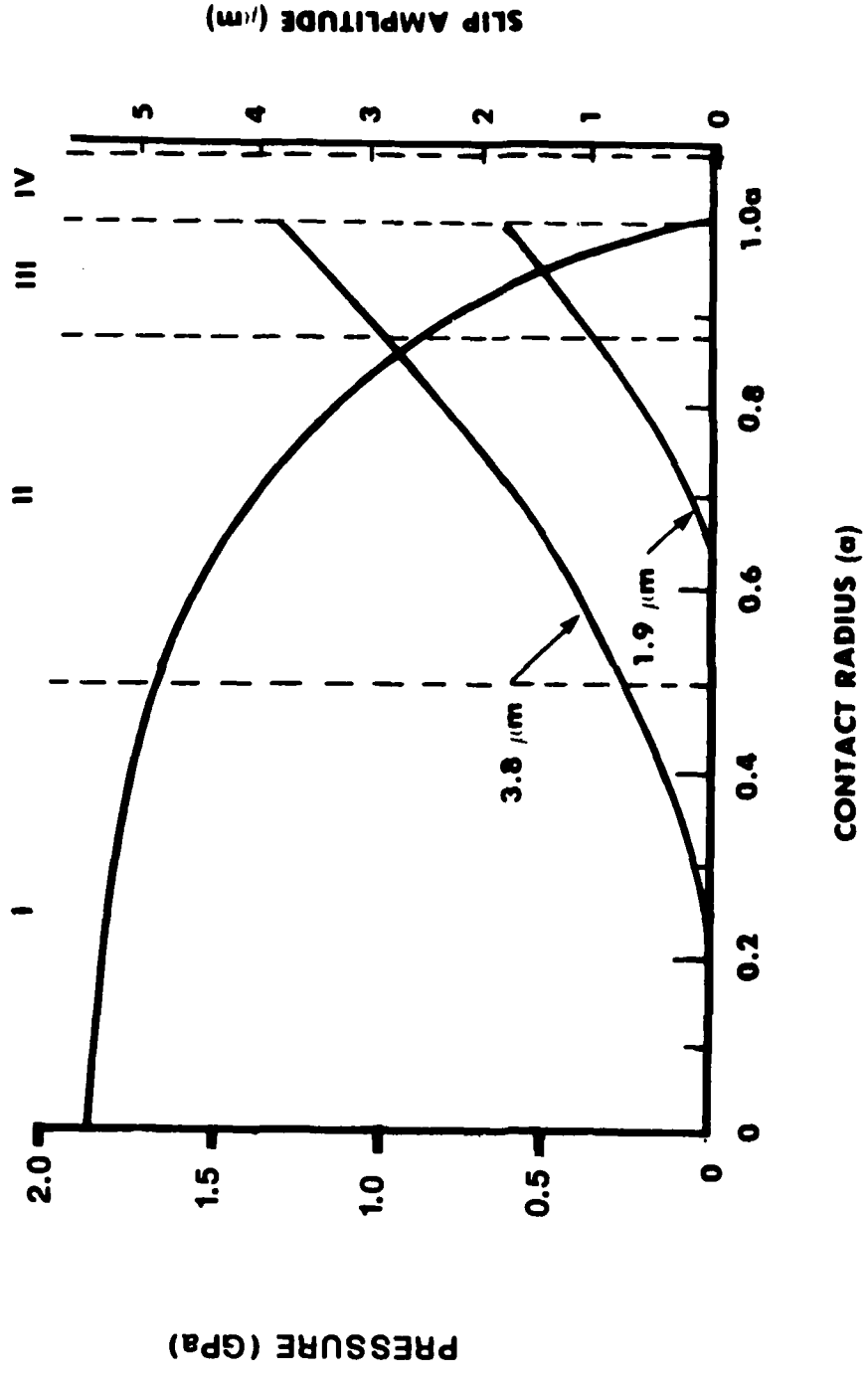

Figure 12 - Composite plot showing pressures distribution and amounts of slip as a function of contact radius (a). Slip was estimated for applied amplitudes of 1.9 and 3.8 μm.

Dr. H. Leidheiser, Jr. 1
Center for Coatings and Surface Research
Lehigh University
Bethlehem, PA 18015

Dr. M. Kendig 1
Rockwell International Science Center
1049 CAmino Dos Rios, P.O. Box 1085
Thousand Oaks, CA 91360

Dr. C. McMahon, LRSM 1
University of Pennsylvania
Philadelphia, PA 19104

Williams Research 1
P. Nagy
Wm. P. Schimmel
2280 W. Maple Blvd.
Walled Lake, MI 48088

National Bureau of Standards 1
Washington, DC 20234

Howmet Turbine Components Corp. 1
475 Steamboat Road
Greenwich, CT 06830

International Nickel Co. 1
R. Benn
Huntington, WV 25720

LTV Aerospace and Defense Company 1
Vought Missiles and Adv. Prgs. Div.
M/S TH-83: C. M. Standard
P.O. Box 650003
Dallas, TX 75265-0003

Martin Marietta 1
C. H. Lund
15 N. Windsor St.
Arlington Heights, IL

Solar Turbines Inc. 1
A. G. Metcalfe
P.O. Box 85376
San Diego, CA 92138-5376

Teledyne CAE 1
Matls. Dev. and Mfg. Engr.
R. Beck
P.O. Box 6971
Toledo, OH 43612

United Technologies Corporation 1
Pratt & Whitney Aircraft
M. Gell
D. Duhl
400 Main St.
East Hartford, CT 06108

United Technologies Corporation 1
J. Moore
M. M. Allen
P.O. Box 2691
West Palm Beach, FL 33402

United Technologies Research Center 1
E. Thompson
F. Lemkey
400 Main Street
East Hartford, CT 06108

Curtis Wright Company 1
Wright Aeronautical Division
J. Mogul
R. Yellin
1 Passaic St.
Wood-Ridge, NJ 07075

Duradyne Tech, Inc. 1
C. Phipps
8607 Tyler Blvd.
Mentor, OH 44060

Garrett Turbine Engine Co. 1
Division of Garrett Corporation
G. Hoppin, III
T. Strangman
111 S. 34th Street — P.O. Box 5217
Phoenix, AZ 85010

General Electric Company 1
Aircraft Engine Business Group
M87/ R. E. Allen
M87/ J. Erickson
1 Neuman Way
Evandale, OH 45215

General Electric Company 1
Corporate R&D Center
G. Benz
M. F. Henry
P.O. Box 8
Schenectady, NY 12301

General Motor Corporation 1
Detroit Diesel Allison
M. Herman
M. Doner
P.O. Box 894
Indianapolis, IN 4206

Howmet Corporation 1
Technical Center
L. Dardi
G. Bouse
699 Benston Rd.
Whitehall, MI 49461

Howmet Turbine Components 1
J. Mihalisin
P.O. Box 371
Dover, NY 07801

National Science Foundation 1
1800 G Street
Washington, DC 20550

U.S. Department of Energy 1
Division of Reactor Research & Tech.
Mail Station B-107: A. Van Echo
Washington, D.C. 20545

Columbia University 1
Professor J. K. Tien
Seely W. Mudd Building
New York, NY 10027

ITT Research Institute 1
S. Verma
S. Firstman
10 West 35th Street
Chicago, IL 60616

Metals and Ceramics Information Ctr. 1
505 King Ave.
Columbus, OH 43201

Southwest Research Institute 1
G. R. Leverant
San Antonio, TX

AVCO R&D 1
201 Lowell Street
Wilmington, MA 01887

AVCO Lycoming Division 1
L. Fiedler
550 S. Main Street
Stratford, CT 06497

Bell Aerosystem Company 1
P.O. Box 1
Buffalo, NY 14240

Cabot Company 1
Satellite Division
J. Klein
P.O. Box 746
Kokomo, IN 46901

Cannon-Muskegon Corp. 1
R. Quigg
G. Erickson
P.O. Box 506
Muskegon, MI 49443

Air Force Office of Scientific Res. 1
Code AFOSR/NE: I. Caplan
Bldg. #417, Bolling AFB
Washington, DC 20332

U.S. Army Mat'ls & Mech. Res. Ctr. 1
Code SLCMT-MCM-SB: P. Farrel
Watertown, MA 02172

U.S. Army Tank Automotive Command
Code AMSTA-RCKM: B. Roopchand
Research and Development Center
Warren, MI 48090

U.S. Army Applied Technology Labs. 1
Code DAVDL-ATL-ATP: J. Lane
Fort Eustis, VA 23604

U.S. Army Missile Command 1
Redstone Arsenal, AL 35809

U.S. Army Research Office 1
Metallurgy & Ceramics Division
Box CM, Duke Station
Durham, NC 27706

Defense Adv. Res. Project Agency 1
Code 641: B. A. Wilcox
1400 Wilson Blvd.
Arlington, VA 22209

NASA/Lewis Research Center 1
Mail Stop [illegible] R. Dreshfield
Mail Stop [illegible]-1: M. Nathal
21000 Brookpark Rd.
Cleveland, OH 44135

NASA/Marshall Space Flight Center 1
Mail Stop EH23: B. Bhat
Huntsville, AL 35812

NASA
RP/ F. Stephenson 1
600 Independence Ave., S.W.
Washington, DC 20546

National Academy of Sciences 1
National Materials Advisory Board
J. C. Lane
2101 Constitution Ave.
Washington, DC 20418

Commander 1
Naval Air Propulsion Center
Code PE34: J. Lawerence Palcza
Code PE43: Mr. Joseph Glatz
1440 Parkway Ave.
Trenton, NJ 08628

Commander 1
Naval Weapons Center
Code 5516
China Lake, CA 93555

Commander 1
Naval Weapons Laboratory
W. Manschreck
Dahlgren, VA 22448

Commander 1
Naval Surface Weapons Center
Metallurgy Division
Code R32: D. Devecha
White Oak
Silver Spring, MD 20910

Commander 1
Naval Sea Systems Command
Code 56X31: R. F. Wyvill
National Center 4, Room #368
Washington, DC 20352

Office of Naval Research 1
Metallurgy Program
Code 471: B. J. McDonald
800 N. Quincy Street
Arlington, VA 22217

Commander 1
Naval Research Laboratory
Code 6395: J. Sprague
Washington, DC 20375

Air Force Wright Aero Lab 1
Code AFWAL/MLLM: N. Geyer
Wright-Patterson AFB, OH 45433

Air Force Wright Aero Lab 1
Code AFWAL/MLTM: S. Lee
Wright-Patterson AFB, OH 45433

Air Force Wright Aero Lab 1
Code AFWAL/POTC: T. Fecke
Wright-Patterson AFB, OH 45433

DISTRIBUTION LIST

REPORT NO. NADC-87036-60

	No. of Copies
Naval Air Systems Command (*00D4*) Washington, DC 20361 (2 for retention) (1 for AIR-5304C1) (1 for AIR-5002C) (1 for AIR-530B31) (1 for AIR-530T) (1 for AIR 931A)	7
Naval Air Rework Facility (Code 343) North Island, San Diego, CA 92135	1
Naval Rework Facility (Code 332) Cherry Point, NC 28533	1
Naval Air Rework Facility (Code 340) Pensacola, FL 32508	1
Naval Air Rework Facility (Code 332) Norfolk, VA 23511	1
Naval Air Rework Facility (Code 342) Alameda, CA 94501	1
Commander Naval Air Force U.S. Atlantic Fleet Norfolk, VA 23511	1
Commander Naval Air Force U.S. Pacific Fleet Naval Air Station, North Island San Diego, CA 92135	1
Defense Technical Information Center Cameron Station, Bldg. 5 Alexandria, VA 22314	12
FAA HQ TRS 2100 2nd St. S.W. Washington, DC 20591	1
David Taylor Naval Ship R & D Center (Code 2812) Annapolis, MD 21402	1
NAVAIRDEVCEN (3 for Code 8131) (16 for Code 6061, Paul Kennedy)	19